

Chapter 13

Beyond the mean-field approximation

In this Chapter we examine how correlation effects beyond the mean-field or Hartree-Fock (HF) picture can be included, by considering the next higher-order contribution to the self-energy of a particle in the medium. We recall that in the self-consistent formulation of Ch. 10 the self-energy is related to the vertex function Γ through the master equation Eq. (10.31). The HF approximation in Ch. 11 was obtained directly from Eq. (10.31) by setting the vertex function $\Gamma = 0$. In terms of diagrams, we had to consider the lowest-order contributions to the self-energy in Fig. 10.2 [and Fig. 10.6a) if an auxiliary potential U is employed]. The self-consistent treatment of these diagrams, indicated by the Dyson equation in Fig. 11.1, was shown to be equivalent to the HF formalism.

The HF self-energy does not depend on energy, and on several occasions we pointed out the shortcomings of such an approach: some specific features of interacting many-body systems cannot be explained by a static self-energy, but require explicit energy-dependence. Energy-dependence appears in the self-energy for the first time when contributions of second order in the interaction are considered. These are listed in Figs. 10.3-10.5 and in Fig. 10.6b)-e). Upon inspection, the diagrams in Fig. 10.3 and Fig. 10.6c)-e) are all reducible, whereas the diagrams in Fig. 10.4 and Fig. 10.6b) are already generated by the HF approximation. So the diagram in Fig. 10.5 - sometimes called *the* second-order diagram, or the Born approximation to the self-energy - is the only genuinely new contribution.

The present Chapter deals exclusively with this second-order diagram, mainly because its energy-dependence is archetypical for all higher-order contributions and therefore warrants a careful analysis.

13.1 The second-order self-energy

The second-order diagram was evaluated in the caption of Fig. 10.5, on the basis of the Feynman rules for the sp propagator developed in Ch. 9. The intermediate fermion lines in the diagram of Fig. 10.5 represent sp propagators $G^{(0)}$ corresponding to a non-interacting system with Hamiltonian $\hat{H}_0 = \hat{T} + \hat{U}$, where \hat{U} is an arbitrary auxiliary potential.

In keeping with our self-consistent formulation, we should now replace the propagators $G^{(0)}$ with interacting propagators,

$$\Sigma^{(2)}(\gamma, \delta; E) = -\frac{1}{2} \int \frac{dE_1}{2\pi i} \int \frac{dE_2}{2\pi i} \sum_{\lambda, \epsilon, \theta} \sum_{\zeta, \xi, \mu} \langle \gamma \lambda | V | \epsilon \theta \rangle \langle \zeta \xi | V | \delta \mu \rangle G(\epsilon, \zeta; E_1) G(\theta, \xi; E_2) G(\mu, \lambda; E_1 + E_2 - E), \quad (13.1)$$

where G is the sp propagator that solves the Dyson equation indicated in Fig. 13.1:

$$G(\alpha, \beta; E) = G^{(0)}(\alpha, \beta; E) + \sum_{\gamma \delta} G(\alpha, \gamma; E) \Sigma(\gamma, \delta; E) G^{(0)}(\delta, \beta; E), \quad (13.2)$$

with the irreducible self-energy

$$\Sigma(\gamma, \delta; E) = -\langle \gamma | U | \delta \rangle + \Sigma^{(1)}(\gamma, \delta) + \Sigma^{(2)}(\gamma, \delta; E), \quad (13.3)$$

now containing the second-order self-energy $\Sigma^{(2)}$ from Eq. (13.1), in addition to the static first-order contribution

$$\Sigma^{(1)}(\gamma, \delta) = -i \int_{C^\dagger} \frac{dE'}{2\pi} \sum_{\mu\nu} \langle \gamma \mu | V | \delta \nu \rangle G(\nu, \mu; E'), \quad (13.4)$$

already analyzed in Ch. 11 [see Eq. (11.11)].

Note that the self-energy in Eq. (13.3) is precisely the expression one gets by setting in Eq. (10.31) the vertex function Γ equal to the free interparticle interaction V ,

$$\langle \zeta \rho | \Gamma(E_1, E_2; E_3, E_4) | \delta \sigma \rangle \equiv \langle \zeta \rho | V | \delta \sigma \rangle. \quad (13.5)$$

The approximation in Fig. (13.1) thus corresponds to replacing the dressed interaction Γ (which includes all in-medium scattering processes) with the free interaction V , and is therefore sometimes called the Born approximation in this context.

By now it should be clear that the self-consistent formulation in Eqs. (13.1) - (13.4) is independent of the auxiliary potential U , since the

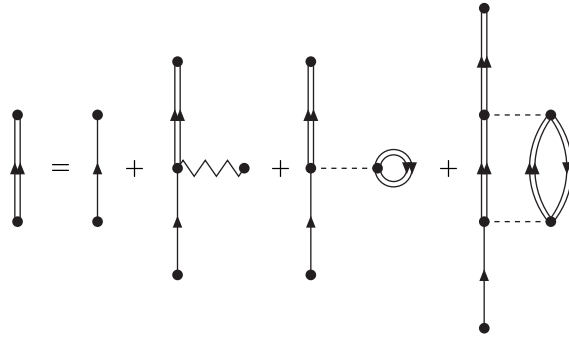


Fig. 13.1 Diagrammatic representation of the second-order Dyson equation.

first term in Eq. (13.3) cancels the U -dependence of the unperturbed propagator $G^{(0)}$. Also note that the first-order contribution in Eq. (13.4) will in general be different from the HF mean field, since the propagator G solves the second-order Dyson equation in Eq. (13.2) rather than the HF equation (11.5).

For a further analysis of the self-energy in Eq. (13.1) the same procedure as for the HF self-energy in Sec. 11.1.1 can be used : we introduce the Lehmann representation of the sp propagator G as

$$G(\alpha, \beta; E) = \sum_m \frac{z_\alpha^{m+} z_\beta^{m+*}}{E - \varepsilon_m^+ + i\eta} + \sum_n \frac{z_\alpha^{n-} z_\beta^{n-*}}{E - \varepsilon_n^- + i\eta}, \quad (13.6)$$

and evaluate the double energy integration in Eq. (13.1) by complex contour integration.

The integrals¹ one encounters are of the form

$$I(E) = \int_{-\infty}^{+\infty} \frac{dE'}{2\pi i} \left(\frac{F_1}{E' - f_1 + i\eta} + \frac{B_1}{E' - b_1 - i\eta} \right) \left(\frac{F_2}{E' - E - f_2 + i\eta} + \frac{B_2}{E' - E - b_2 - i\eta} \right). \quad (13.7)$$

The integration contour along the real axis can be closed by including a large semicircle in the upper or lower complex E' half plane. Since the integrand behaves as $|E'|^{-2}$ for $|E'| \rightarrow +\infty$, such a semicircle (in the limit of infinite radius) yields a vanishing contribution to the integral, and its inclusion does not change the result. The product in Eq. (13.7) has four terms. However, the $F_1 F_2$ and $B_1 B_2$ terms have two poles in the same

¹The contour integrals needed for this book never get more complicated than this.

(upper or lower) half plane and do not contribute to the integral, as can be seen by closing the contour with a semicircle in the opposite half plane. The F_1B_2 and F_2B_1 terms have a pole in both halfplanes, and contribute, according to the residue theorem, as

$$I(E) = \frac{F_1B_2}{E - (f_1 - b_2) + i\eta} - \frac{B_1F_2}{E + (f_2 - b_1) - i\eta}. \quad (13.8)$$

The self-energy in Eq. (13.1) is easily evaluated by repeated use of Eq. (13.8) and reads

$$\begin{aligned} \Sigma^{(2)}(\gamma, \delta; E) = & \frac{1}{2} \sum_{\lambda, \epsilon, \theta} \sum_{\zeta, \xi, \mu} \langle \gamma \lambda | V | \epsilon \theta \rangle \langle \zeta \xi | V | \delta \mu \rangle \\ & \left(\sum_{m_1 m_2 n_3} \frac{z_\epsilon^{m_1+} z_\zeta^{m_1+*} z_\theta^{m_2+} z_\xi^{m_2+*} z_\mu^{n_3-} z_\lambda^{n_3*}}{E - (\varepsilon_{m_1}^+ + \varepsilon_{m_2}^+ - \varepsilon_{n_3}^-) + i\eta} \right. \\ & \left. + \sum_{n_1 n_2 m_3} \frac{z_\epsilon^{n_1-} z_\zeta^{n_1-*} z_\theta^{n_2-} z_\xi^{n_2-*} z_\mu^{m_3+} z_\lambda^{m_3+*}}{E + (\varepsilon_{m_3}^+ - \varepsilon_{n_1}^- - \varepsilon_{n_2}^-) - i\eta} \right). \end{aligned} \quad (13.9)$$

We recall (see Sec. 8.3) that the poles of the sp propagator in Eq. (13.6) belong either to the particle addition (ε_m^+) or removal (ε_n^-) domain,

$$\forall m, n : \varepsilon_n^- \leq \varepsilon_F^- < \varepsilon_F < \varepsilon_F^+ \leq \varepsilon_m^+, \quad (13.10)$$

which are separated by the Fermi energy

$$\varepsilon_F = \frac{1}{2}[\varepsilon_F^- + \varepsilon_F^+]. \quad (13.11)$$

As a consequence, the poles appearing in the the second-order self-energy of Eq. (13.9) obey the inequalities

$$\forall m_i, n_i : \varepsilon_{n_1}^- + \varepsilon_{n_2}^- - \varepsilon_{m_3}^+ < \varepsilon_F < \varepsilon_{m_1}^+ + \varepsilon_{m_2}^+ - \varepsilon_{n_3}^-. \quad (13.12)$$

This feature also holds in higher orders, and in general the energy-dependent part of the self-energy has the same analytic structure as the sp propagator G : a sum of simple poles, shifted slightly off the real axis into the lower (upper) half plane for poles corresponding to the addition (removal) domain.

13.2 Solution of the Dyson equation

Before proceeding in Sec.13.4 with the full self-consistent treatment indicated in Fig. 13.1, it is instructive first to examine how the Dyson equation is modified by the presence of energy-dependent terms in the self-energy. To simplify matters we evaluate the self-energy in Eq. (13.3) with HF propagators and set the auxiliary potential U equal to the HF potential [i.e. $G^{(0)} \equiv G^{HF}$ in Eq. (13.2)]. This can also be considered as a first iteration when solving the full self-consistency problem. We choose the HF sp basis, so the HF propagator,

$$G^{HF}(\alpha, \beta; E) = \delta_{\alpha, \beta} \left[\frac{\theta(\alpha - F)}{E - \varepsilon_\alpha + i\eta} + \frac{\theta(F - \alpha)}{E - \varepsilon_\alpha - i\eta} \right], \quad (13.13)$$

is diagonal in the sp labels.

To find the corresponding second-order self-energy we simply have to set

$$z_\alpha^{m+} = \delta_{m, \alpha} \theta(\alpha - F); \quad z_\alpha^{n-} = \delta_{n, \alpha} \theta(F - \alpha), \quad (13.14)$$

in the general expression (13.9). The resulting self-energy reads

$$\begin{aligned} \Sigma^{(2)}(\gamma, \delta; E) = & \frac{1}{2} \sum_{\lambda, \epsilon, \theta} \langle \gamma \lambda | V | \epsilon \theta \rangle \langle \epsilon \theta | V | \delta \lambda \rangle \\ & \left(\frac{\theta(\epsilon - F) \theta(\nu - F) \theta(F - \lambda)}{E - (\varepsilon_\epsilon + \varepsilon_\nu - \varepsilon_\lambda) + i\eta} \right. \\ & \left. + \frac{\theta(F - \epsilon) \theta(F - \nu) \theta(\lambda - F)}{E + (\varepsilon_\lambda - \varepsilon_\epsilon - \varepsilon_\nu) - i\eta} \right), \end{aligned} \quad (13.15)$$

or, in a more compact notation,

$$\begin{aligned} \Sigma^{(2)}(\gamma, \delta; E) = & \frac{1}{2} \left(\sum_{p_1 p_2 h_3} \frac{\langle \gamma h_3 | V | p_1 p_2 \rangle \langle p_1 p_2 | V | \delta h_3 \rangle}{E - (\varepsilon_{p_1} + \varepsilon_{p_2} - \varepsilon_{h_3}) + i\eta} \right. \\ & \left. + \sum_{h_1 h_2 p_3} \frac{\langle \gamma p_3 | V | h_1 h_2 \rangle \langle h_1 h_2 | V | \delta p_3 \rangle}{E + (\varepsilon_{p_3} - \varepsilon_{h_1} - \varepsilon_{h_2}) - i\eta} \right), \end{aligned} \quad (13.16)$$

where labels identifying particle (p) and hole (h) states in the HF approximation have been introduced. We will proceed to examine the solution G

of the equation

$$G(\alpha, \beta; E) = G^{HF}(\alpha, \beta; E) + \sum_{\gamma\delta} G(\alpha, \gamma; E) \Sigma^{(2)}(\gamma, \delta; E) G^{HF}(\delta, \beta; E). \quad (13.17)$$

13.2.1 Diagonal approximation

It is clear from Eq. (13.16) that the second-order self-energy in principle has non-diagonal contributions, even when evaluated with the diagonal HF sp propagator. However, in some cases it is a good approximation to neglect the off-diagonal terms. This happens e.g. in closed-shell nuclei, where off-diagonal elements would require mixing between major shells having a large energy separation.

Within this diagonal approximation, the self-energy (13.16) reads

$$\Sigma^{(2)}(\alpha; E) = \frac{1}{2} \left(\sum_{p_1 p_2 h_3} \frac{|\langle \alpha h_3 | V | p_1 p_2 \rangle|^2}{E - (\varepsilon_{p_1} + \varepsilon_{p_2} - \varepsilon_{h_3}) + i\eta} + \sum_{h_1 h_2 p_3} \frac{|\langle \alpha p_3 | V | h_1 h_2 \rangle|^2}{E + (\varepsilon_{p_3} - \varepsilon_{h_1} - \varepsilon_{h_2}) - i\eta} \right), \quad (13.18)$$

and the Dyson equation (13.17) becomes

$$G(\alpha; E) = G^{HF}(\alpha; E) + G(\alpha; E) \Sigma^{(2)}(\alpha; E) G^{HF}(\alpha; E). \quad (13.19)$$

The latter has a simple algebraic solution,

$$G(\alpha; E) = \frac{1}{\frac{1}{G^{HF}(\alpha; E)} - \Sigma^{(2)}(\alpha; E)} = \frac{1}{E - \varepsilon_\alpha - \Sigma^{(2)}(\alpha; E)}. \quad (13.20)$$

For the last identity we used the inverse of the HF propagator in Eq. (13.13) [the infinitesimal $\pm i\eta$ are irrelevant when they do not appear in the denominator of a pole term],

$$\frac{1}{G^{HF}(\alpha; E)} = E - \varepsilon_\alpha. \quad (13.21)$$

Extracting physical information from the sp propagator in general requires the knowledge of its poles and residues (see Sec. 8.3). For the propagator $G(\alpha; E)$ given by the formal solution in Eq. (13.20), the poles $E_{n\alpha}$

obviously correspond to the roots of the non-linear equation

$$E_{n\alpha} = \varepsilon_\alpha + \Sigma^{(2)}(\alpha; E_{n\alpha}), \quad (13.22)$$

with $\Sigma^{(2)}(\alpha; E)$ defined in Eq. (13.18). The residue $R_{n\alpha}$ at the pole $E_{n\alpha}$ of the propagator follows from

$$\begin{aligned} R_{n\alpha} &= \lim_{E \rightarrow E_{n\alpha}} (E - E_{n\alpha})G(\alpha; E) = \lim_{E \rightarrow E_{n\alpha}} \frac{E - E_{n\alpha}}{E - \varepsilon_\alpha - \Sigma^{(2)}(\alpha; E)} \\ &= \left(1 - \frac{d\Sigma^{(2)}(\alpha; E)}{dE} \Big|_{E=E_{n\alpha}} \right)^{-1}. \end{aligned} \quad (13.23)$$

Note that, when determining the roots of Eq. (13.22), the infinitesimal $\pm i\eta$ appearing in the denominator of Eq. (13.18) can again be omitted, provided that the self-energy has poles at a set of discrete energies (i.e. a set of isolated simple poles). In principle the $\pm i\eta$ generate, according to Eq.(8.15), an imaginary part of the self-energy consisting of a sequence of δ -functions located at these discrete energies; since discrete solutions to Eq. (13.22) cannot coincide with a pole of the self-energy, the δ -functions do not influence the position of the roots of Eq. (13.22), which are all real. This does not hold when the self-energy has a continuous distribution of poles (which is equivalent to a branch cut), as will be clarified in the discussion on infinite systems in Sec. 13.3).

To gain insight in the location of the roots of Eq. (13.22), a graphical solution of the Dyson equation is often helpful. In Fig. 13.2 the energy-dependence of the self-energy $\Sigma^{(2)}(\alpha; E)$ of Eq. (13.18) is shown. The case on display is for a typical confined finite system, having a discrete HF spectrum. The hole and particle HF energies are separated by the particle-hole gap, which has a width $\Delta = \varepsilon_p^{min} - \varepsilon_h^{max}$ and is centered on the HF Fermi energy,

$$\varepsilon_F = \frac{1}{2}(\varepsilon_p^{min} + \varepsilon_h^{max}). \quad (13.24)$$

Since the poles in Eq. (13.18) all have positive residues, $\Sigma^{(2)}(\alpha; E)$ is monotonically decreasing where defined. There is a sequence of simple poles in the addition domain, located at the unperturbed HF $2p1h$ energies, and another sequence in the removal domain, located at (minus) the unperturbed HF $2h1p$ energies. The poles of the addition and removal sequence are separated by a gap of (at least) three times the HF particle-hole gap.

Fig. 13.2 Example of second-order self-energy in Eq. (13.18).

The roots of Eq. (13.22) are simply the intersection points of the self-energy $\Sigma^{(2)}(\alpha; E)$ with the straight line $E - \varepsilon_\alpha$. It is obvious from the graph in Fig. 13.2 that between any two successive poles of the self-energy a root is located. In addition, there is a root to the left and right of the sequence of self-energy poles. When a finite sp basis set is used, this implies that a self-energy having D poles leads to a sp propagator with $D + 1$ poles.

The interpretation of these roots should by now be straightforward. The poles $E_{n\alpha}$ in the removal domain (below the Fermi energy) must be interpreted as approximate energies of the eigenstates in the $N - 1$ system,

$$E_{n\alpha} \approx E_0^N - E_n^{N-1}, \quad (13.25)$$

that can be obtained by removing a particle in the sp state α from the N -particle ground state. The residue then corresponds to the (squared) removal amplitude,

$$R_{n\alpha} \approx |\langle \Psi_n^{N-1} | a_\alpha | \Psi_0^N \rangle|^2. \quad (13.26)$$

Similarly, the poles $E_{n\alpha}$ in the addition domain (above the Fermi energy) correspond to eigenstates in the $N + 1$ system,

$$E_{n\alpha} \approx E_n^{N+1} - E_0^N, \quad (13.27)$$

having addition amplitudes

$$R_{n\alpha} \approx |\langle \Psi_n^{N+1} | a_\alpha^\dagger | \Psi_0^N \rangle|^2. \quad (13.28)$$

Note that since $d\Sigma^{(2)}(\alpha; E)/dE < 0$, the residues $R_{n\alpha}$ that follow from

Eq. (13.23) obey

$$0 \leq R_{n\alpha} \leq 1, \quad (13.29)$$

in accordance with their relation to the physical addition or removal amplitudes.

All of this means that adding the energy-dependent second-order self-energy to the static HF self-energy produces quite dramatic effects. The removal from the ground state of a particle in an occupied HF sp state α no longer leads to a unique $N - 1$ state, as predicted in the HF picture, but rather to a large number of $N - 1$ states, each having a finite removal amplitude. Moreover, the removal from the ground state of a particle in an unoccupied HF sp state α - clearly impossible in HF - is now allowed. Similar statements hold in the addition domain. Of course, any more sophisticated treatment of the self-energy will also include these fragmentation effects on the sp strength. Experimental information on physical spectral functions indicate that such features are indispensable for a meaningful comparison with data.

As a final remark on Fig. 13.2, we note that if the unperturbed sp energy ε_α is not too far removed from the Fermi energy, the root of Eq. (13.22) lying in the interval which separates the removal and addition domain is somewhat special: since the self-energy $\Sigma^{(2)}(\alpha; E)$ has no poles in this interval, the energy derivative is small in this region, and as a consequence the residue corresponding to this root will be quite close to (but still smaller than) unity. Such a solution represents a quasiparticle or quasihole excitation in a finite system, and corresponds to a $N \pm 1$ eigenstate which has a rather pure sp character. On the other hand, if the sp energy ε_α is far from the Fermi energy, it is in a region where the density of $2p1h$ or $2h1p$ states is high, and the sp strength of this orbital will be strongly fragmented over many $N - 1$ states. The different fragmentation pattern observed for valence hole and deeply bound hole states in finite nuclei is readily understood by these elementary considerations.

13.2.2 *Link with perturbation theory*

As shown in Ch. 11, the HF formalism assumes that the N -particle ground state is the HF Slater determinant,

$$(\text{HF:}) \quad |\Psi_0^N\rangle \approx |\Phi_{HF}^N\rangle = \prod_{h=1}^N |0\rangle. \quad (13.30)$$

and that the eigenstates of the $N + 1$ system are simple $1p$ excitations,

$$(\text{HF:}) \quad |\Psi_p^{N+1}\rangle \approx a_p^\dagger |\Phi_{HF}^N\rangle. \quad (13.31)$$

Corrections to this picture can be obtained by allowing admixtures with $2p1h$ excitations,

$$|\Psi_p^{N+1}\rangle \approx x a_p^\dagger |\Phi_{HF}^N\rangle + \sum_{p_1 < p_2} \sum_{h_3} X_{p_1 p_2 h_3} a_{p_1}^\dagger a_{p_2}^\dagger a_{h_3} |\Phi_{HF}^N\rangle. \quad (13.32)$$

The eigenstates in this basis are found by diagonalization of the Hamiltonian matrix,

$$\begin{pmatrix} \varepsilon_p & \mathcal{V} \\ \mathcal{V}^\dagger & \mathcal{E} \end{pmatrix} \begin{pmatrix} x \\ X \end{pmatrix} = E \begin{pmatrix} x \\ X \end{pmatrix}, \quad (13.33)$$

where \mathcal{V} contains the coupling between $1p$ and $2p1h$ configurations,

$$\mathcal{V}_{p_1 p_2 h_3} = \langle \Phi_{HF}^N | a_p \hat{H} a_{p_1}^\dagger a_{p_2}^\dagger a_{h_3} | \Phi_{HF}^N \rangle = \langle ph_3 | V | p_1 p_2 \rangle. \quad (13.34)$$

Under the assumption (typical in perturbation theory) that the $2p1h$ configurations do not interact among themselves, we have

$$\begin{aligned} \mathcal{E}_{p_1 p_2 h_3, p'_1 p'_2 h'_3} &= \langle \Phi_{HF}^N | a_{h'_3}^\dagger a_{p_2} a_{p_1} \hat{H} a_{p_1}^\dagger a_{p_2}^\dagger a_{h_3} | \Phi_{HF}^N \rangle \\ &\approx \delta_{p_1, p'_1} \delta_{p_2, p'_2} \delta_{h_3, h'_3} (\varepsilon_{p_1} + \varepsilon_{p_2} - \varepsilon_{h_3}). \end{aligned} \quad (13.35)$$

Elimination of X from Eq. (13.33) then leads to

$$X = \frac{1}{E - \mathcal{E}} \mathcal{V}^\dagger x, \quad (13.36)$$

$$E x = \left(\varepsilon + \mathcal{V} \frac{1}{E - \mathcal{E}} \mathcal{V}^\dagger \right) x. \quad (13.37)$$

According to Eq. (13.37), the eigenenergies for states with $x \neq 0$ (i.e. states that have a nonvanishing overlap with the $1p$ state $a_p^\dagger |\Phi_{HF}^N\rangle$) are therefore the roots of

$$E = \varepsilon_p + \sum_{p_1 < p_2, h_3} \frac{|\langle ph_3 | V | p_1 p_2 \rangle|^2}{E - (\varepsilon_{p_1} + \varepsilon_{p_2} - \varepsilon_{h_3})}. \quad (13.38)$$

This is seen to be analogous to Eq. (13.22), but only the forward ($2p1h$) term of the self-energy in Eq. (13.18) is generated, as a consequence of the unperturbed HF ground state (13.30) appearing in the ansatz of Eq. (13.32). In contrast, the Green function formalism which led to Eq. (13.22) automatically builds in ground-state correlations, in a single coherent framework for both the $N + 1$ and $N - 1$ excited states.

13.2.3 Sumrules

The analytic structure of Eqs. (13.18-13.22), generated by the second-order diagram, is in fact quite general and also appears in more complicated cases, when higher-order diagrams or an infinite resummation of a subclass of diagrams are included in the self-energy. It is therefore worthwhile to examine the properties of the generical expression

$$G(E) = \frac{1}{E - \varepsilon - \Sigma(E)}, \quad (13.39)$$

where both the propagator $G(E)$ and the self-energy $\Sigma(E)$ are a sum of simple poles,

$$\Sigma(E) = \sum_n \frac{s_n}{E - \omega_n}, \quad G(E) = \sum_N \frac{S_N}{E - \Omega_N}. \quad (13.40)$$

Analogous to Eq. (13.22), the Ω_N are the roots of

$$\Omega_N - \varepsilon = \sum_n \frac{s_n}{\Omega_N - \omega_n}, \quad (13.41)$$

whereas the sp strength at Ω_N follows [see Eq. (13.23)] from

$$S_N = \frac{1}{1 + \sum_n \frac{s_n}{(\Omega_N - \omega_n)^2}}. \quad (13.42)$$

However, without explicitly solving Eq. (13.41) it is possible to derive sumrules which relate the distribution of sp strength (Ω_N, S_N) with the self-energy strength (ω_n, s_n) and which are often useful as a numerical check on calculated spectral functions.

Considering the leading order in a $(1/E)$ expansion of Eq. (13.39) immediately leads to

$$E \rightarrow \infty \Rightarrow \sum_N S_N = 1. \quad (13.43)$$

This implies, in accordance with the fundamental sumrule in Eq. (8.18), that the summed sp strength is always equal to unity, irrespective of the values of the poles and residues appearing in the self-energy.

Having the energy E in Eq. (13.39) coincide with one of the poles ω_n of the self-energy yields

$$E \rightarrow \omega_n \Rightarrow 0 = \sum_N \frac{S_N}{\Omega_N - \omega_n}, \quad (13.44)$$

whereas the limit $E \rightarrow \Omega_N$ leads back to Eq. (13.41). Combining Eq. (13.44) with Eq. (13.41) we get

$$\sum_N S_N (\Omega_N - \varepsilon) = \sum_N \sum_n \frac{S_N s_n}{\Omega_N - \omega_n} = 0, \quad (13.45)$$

which implies that the centroid of the sp strength distribution is the sp energy ε .

In a similar way, general recursion formula for the higher-order central moments of the sp strength distribution are obtained. Defining

$$M_k = \sum_N (\Omega_N - \varepsilon)^k S_N; \quad m_k = \sum_n (\omega_n - \varepsilon)^k s_n, \quad (13.46)$$

we have $M_0 = 1$ and $M_1 = 0$ [according to Eqs. (13.43) and (13.45)] and for $k \geq 2$,

$$\begin{aligned} M_k &= \sum_N S_N (\Omega_N - \varepsilon)^{k-1} \sum_n \frac{s_n}{\Omega_N - \omega_n} \\ &= \sum_n s_n \sum_N S_N \left[\frac{(\Omega_N - \varepsilon)^{k-1} - (\omega_n - \varepsilon)^{k-1}}{(\Omega_N - \varepsilon) - (\omega_n - \varepsilon)} + \frac{(\omega_n - \varepsilon)^{k-1}}{\Omega_N - \omega_n} \right] \\ &= \sum_{l=0}^{k-2} M_l m_{k-l-2} \end{aligned} \quad (13.47)$$

In particular we find $M_2 = m_0$, i.e. the second central moment, describing the width of the spectral function, is equal to the summed self-energy strength.

Also the moments of negative order M_{-k} (or inverse energy-weighted sumrules) can be obtained by recursion. Considering, for $k \geq 0$,

$$M_{-k} = \sum_N \frac{S_N}{(\Omega_N - \varepsilon)^k} = \sum_N \frac{S_N}{(\Omega_N - \varepsilon)^{k+1}} \sum_n \frac{s_n}{\Omega_N - \omega_n}, \quad (13.48)$$

and using the identity

$$\frac{1}{x^{k+1}(x-y)} = \frac{1}{y^{k+1}(x-y)} - \sum_{l=1}^{k+1} \frac{1}{y^l x^{k-l+2}}, \quad (13.49)$$

with $x = \Omega_N - \varepsilon$ and $y = \omega_n - \varepsilon$, one arrives at

$$M_{-(k+1)} = -\frac{1}{m_{-1}} \left(M_{-k} + \sum_{l=1}^k M_{-l} m_{-(k-l+1)} \right). \quad (13.50)$$

13.2.4 General (non-diagonal) self-energy

We now drop the simplification introduced in Sec. 13.2.1 and consider also the nondiagonal contributions to the self-energy in Eq. (13.16). We will again assume that the self-energy has a set of isolated simple poles and omit the $\pm i\eta$ in the denominator. The Dyson equation can then generically be rewritten as (we use square brackets to emphasize the matrix structure)

$$[G(E)] = (E - [\varepsilon] - [\Sigma(E)])^{-1}, \quad (13.51)$$

where both the propagator and the self-energy are sums over discrete simple poles,

$$[G(E)] = \sum_N \frac{[S_N]}{E - \Omega_N}, \quad [\Sigma(E)] = \sum_n \frac{[s_n]}{E - \omega_n}. \quad (13.52)$$

Note that all matrices have sp labels as indices, and that the matrices $[S_N]$ and $[s_n]$ are hermitian and positive (having real eigenvalues ≥ 0).

The analysis proceeds in much the same way as in Sec. 13.2.1, but some care has to be taken because of the possibly noncommuting matrix quantities. From Eq. (13.51) it is clear that a pole Ω_N of the propagator is a zero eigenvalue appearing in the nonlinear eigenvalue equation

$$\Omega_N X_N = ([\varepsilon] + [\Sigma(\Omega_N)])X_N. \quad (13.53)$$

We allow for the possibility that Ω_N is a degenerate eigenvalue, and write the spectral decomposition as

$$[\varepsilon] + [\Sigma(\Omega_N)] = \Omega_N [P_N] + \sum_M \lambda_M [P_M], \quad (13.54)$$

where the $\lambda_M (\neq \Omega_N)$ are the other eigenvalues of $([\varepsilon] + [\Sigma(\Omega_N)])$ and $[P_N]$, $[P_M]$ are projection operators on the corresponding eigenspaces.

The residue of the propagator $[G(E)]$ at the pole Ω_N is given by

$$\begin{aligned} [S_N] &= \lim_{E \rightarrow \Omega_N} (E - \Omega_N)[G(E)] \\ &= \lim_{\eta \rightarrow 0} \eta (\Omega_N + \eta - [\varepsilon] - [\Sigma(\Omega_N)] - \eta[\Sigma'(\Omega_N)])^{-1}, \end{aligned} \quad (13.55)$$

where the energy-derivative of the self-energy is the negative hermitian matrix

$$[\Sigma'(E)] = - \sum_n \frac{[s_n]}{(E - \omega_n)^2}. \quad (13.56)$$

Using the spectral decomposition Eq. (13.54) one can verify that the matrix

$$[A] = \Omega_N + \eta - [\varepsilon] - [\Sigma(\Omega_N)] = \eta[P_N] + \sum_M (\Omega_N - \lambda_M + \eta)[P_M] \quad (13.57)$$

is invertible for $\eta \neq 0$, the inverse being

$$[A]^{-1} = \frac{1}{\eta}[P_N] + \sum_M \frac{1}{\Omega_N - \lambda_M + \eta}[P_M]. \quad (13.58)$$

The residue $[S_N]$ in Eq. (13.55), rewritten in terms of $[A]^{-1}$, reads

$$[S_N] = \lim_{\eta \rightarrow 0} \eta (1 - \eta[A]^{-1}[\Sigma'(\Omega_N)])^{-1} [A]^{-1}. \quad (13.59)$$

The limit $\eta \rightarrow 0$ can now be safely taken, and since

$$\lim_{\eta \rightarrow 0} \eta[A]^{-1} = [P_N], \quad (13.60)$$

the residue matrix at the pole Ω_N is

$$[S_N] = (1 - [P_N][\Sigma'(\Omega_N)])^{-1} [P_N]. \quad (13.61)$$

It is always possible to choose eigenvectors $X_{N\nu}$ in Eq. (13.53) such that $[P_N] = \sum_{\nu} X_{N\nu} X_{N\nu}^{\dagger}$ and $[\Sigma'(\Omega_N)]$ is diagonal in the $[P_N]$ -subspace,

$$X_{N\nu}^{\dagger} [\Sigma'(\Omega_N)] X_{N\nu'} = -\delta_{\nu,\nu'} u_{N\nu}^2. \quad (13.62)$$

Using this basis, Eq. (13.61) can be reexpressed as

$$[S_N] = \sum_{\nu} \frac{1}{1 + u_{N\nu}^2} X_{N\nu} X_{N\nu}^{\dagger}, \quad (13.63)$$

which clearly shows that the residue matrix $[S_N]$ is indeed a positive hermitian matrix.

At this point it may be good to mention that the above analysis is given primarily for the purpose of mathematical completeness. In the majority of practical applications, the eigenvalue Ω_N in Eq. (13.53) is nondegenerate, i.e. $[P_N] = X_N X_N^{\dagger}$, and Eq. (13.61) simplifies to

$$[S_N] = \frac{1}{1 - X_N^{\dagger} [\Sigma'(\Omega_N)] X_N} X_N X_N^{\dagger}. \quad (13.64)$$

Graphically, the situation is also a bit more complicated than in the diagonal case. The poles of the propagator in Eq. (13.51) can be found by plotting the eigenvalue curves $\lambda_{\nu}(E)$ of the matrix $[\varepsilon] + [\Sigma(E)]$ as a function

Fig. 13.3 Eigenvalue curves of the non-diagonal second-order self-energy as in Eq. (13.65).

of E , and determining the intersection points $\lambda_\nu(E) = E$. As an example, the eigenvalue curves of the matrix

$$\epsilon_\alpha \delta_{\alpha,\beta} + \sum_{n=1}^4 \frac{r_{n\alpha} r_{n\beta}}{E - \omega_n} \quad (13.65)$$

are shown in Fig. 13.3.

The eigenvalue curves in Fig. 13.3 are all monotonously decreasing where defined. This is easily understood by realizing that the energy derivatives follow from first-order perturbation theory,

$$\lambda'_\nu(E) = X_\nu^\dagger(E) [\Sigma'(E)] X_\nu(E) = - \sum_n \frac{X_\nu^\dagger(E) [s_n] X_\nu(E)}{(E - \omega_n)^2} < 0. \quad (13.66)$$

Also note the curious behaviour of the $\lambda_\nu(E)$ near a pole ω_n of the self-energy. Some of the eigenvalues curves have an asymptote, whereas others are regular at ω_n . It turns out that, if d_n is the rank of the residue matrix $[s_n]$ in the self-energy, then d_n of the eigenvalue curves have an asymptote at $E = \omega_n$. This can be seen by introducing the spectral decomposition

$$[\varepsilon] + [\Sigma(E)] = \sum_\nu \lambda_\nu(E) [P_\nu(E)] \quad (13.67)$$

and expressing $[s_n]$ as

$$[s_n] = \lim_{E \rightarrow \omega_n} [\Sigma(E)]$$

$$= \sum_{\nu} \{(E - \omega_n)\lambda_{\nu}(E)\} [P_{\nu}(E)]. \quad (13.68)$$

It follows that one of the eigenvalues $\lambda_{\nu}(E)$, say $\lambda_0(E)$, must behave as $\lambda_0(E) \rightarrow \frac{C}{E - \omega_n}$ in the limit $E \rightarrow \omega_n$, whereas the other eigenvalues are regular at ω_n . The eigenspace corresponding to λ_0 then has a projection operator $[P_0] = \frac{1}{C}[s_n]$, its dimension being equal to the rank of $[s_n]$.

From the graphical analysis it is clear that the total number of poles Ω_N of the propagator in Eq. (13.51) is $M + \sum_n d_n$, where M is the dimension of the sp space. Applied to the second-order self-energy, $\sum_n d_n$ is the dimension of the combined $2p1h$ and $2h1p$ space, where the d_n take possible degeneracies in the spectrum of $2p1h$ or $2h1p$ energies into account. The number of poles in the propagator therefore agrees with what we expect from an eigenvalue problem describing the mixing of sp states with $2p1h$ and $2h1p$ states.

13.3 Infinite systems

13.3.1 Dispersion relations

In the case of an homogeneous infinite system the sp propagator and self-energy are automatically diagonal in the plane-wave basis, as was discussed in Sec. 11.4. The second-order self-energy in Eq. (13.18) becomes ²

$$\Sigma^{(2)}(p; E) = \frac{1}{2} \sum_{\mathbf{p}_1 \mathbf{p}_2 \mathbf{p}_3} |\langle \mathbf{p} \mathbf{p}_3 | V | \mathbf{p}_1 \mathbf{p}_2 \rangle|^2 \times \quad (13.69)$$

$$\left(\frac{\theta(p_1 - k_F)\theta(p_2 - k_F)\theta(k_F - p_3)}{E - [\varepsilon(p_1) + \varepsilon(p_2) - \varepsilon(p_3)] + i\eta} + \frac{\theta(k_F - p_1)\theta(k_F - p_2)\theta(p_3 - k_F)}{E + [\varepsilon(p_3) - \varepsilon(p_1) - \varepsilon(p_2)] - i\eta} \right).$$

The $\varepsilon(p)$ represent HF sp energies, and $\varepsilon_F = \varepsilon(k_F)$ is the HF approximation to the Fermi energy.

The interaction matrix elements in Eq.(13.69) have the form

$$\langle \mathbf{p}_1 \mathbf{p}_2 | V | \mathbf{p}_3 \mathbf{p}_4 \rangle = \frac{1}{V} \delta_{\mathbf{p}_1 + \mathbf{p}_2, \mathbf{p}_3 + \mathbf{p}_4} w(\mathbf{p}_1, \mathbf{p}_2, \mathbf{p}_3, \mathbf{p}_4), \quad (13.70)$$

where w is a continuous function of the sp momenta, V is the normalization volume, and momentum conservation is expressed through the Kronecker- δ .

²For notational simplicity we consider fermions of a single species. The inclusion of spin or isospin degrees of freedom does not change the present considerations.